JOURNAL OF COMPUTATIONAL PHYSICS 16, 259–270 (1974)

A Finite-Difference Newton–Raphson Solution of the Two-Center Electronic Schrödinger Equation

J. K. CAYFORD, W. R. FIMPLE, D. G. UNGER, AND S. P. WHITE

Department of Physics, University of Canterbury, Christchurch, New Zealand

Received June 4, 1974

An alternative approach to the solution of the two-center electronic Schrödinger equation involving a finite-difference Newton–Raphson algorithm is described. The usual separation in confocal elliptical coordinates is employed leading to two coupled one-dimensional differential equations with split boundary conditions. The corresponding set of finite-difference equations, including the energy eigenvalue, separation constant, boundary conditions, and normalization conditions, are incorporated into a large system of nonlinear algebraic equations which is solved by means of a generalized Newton–Raphson iteration. The present algorithm is relatively simple and flexible. Solutions at one value of the nuclear separation can be easily tracked into solutions at other values. Also with a modification of the boundary conditions continuum states can be obtained as easily as bound states. As examples, calculations of the $2s\sigma_g$ bound state and a positive-energy continuum state of H_2^+ at a separation $R = 5.0$ AU are presented. Through the use of a generalized Richardson extrapolation an accuracy of eight significant figures has been achieved.

1. INTRODUCTION

It is well known that the two-center electronic Schrödinger equation separates in confocal elliptical coordinates λ, μ, ϕ. This separation is generally attributed to Burrau [1], and the standard truncated infinite series method of solving the resulting coupled ordinary differential equations with split boundary conditions has been widely used [2–6]. Very accurate wavefunctions for H_2^+ are available [6].

The usefulness of the single-electron diatomic orbitals as basis functions in calculations of stationary electronic states of larger molecules and in calculations of atom–atom collisions is another question. Wallis and Hulburt [4] reported the difficulties of using the standard diatomic orbitals as basis functions for larger diatomic molecules. One of the difficulties is the fact that as the central nuclear charges increase the convergence of the infinite series becomes rapidly worse. But more importantly, the continuum states, which are generally neglected,

may make a significant contribution. This latter difficulty has been overcome by Llaguno, Gupta, and Rothstein [7] who used elliptic-type-orbitals (the elliptic analogs of Slater-type orbitals) in calculations on H_2^+, H_2, He_2^{2+}, and H_3^+.

In the present paper a finite-difference Newton–Raphson algorithm is used to solve the two-center electronic Schrödinger equation. In a previous paper [8] this method has been employed to solve the atomic Hartree–Fock equations. In general this algorithm is very powerful in solving sets of coupled ordinary differential equations with split boundary conditions.

With the finite-difference method two-center orbitals can be generated easily and quickly for a wide range of nuclear separations and charges. Also, with an appropriate change of boundary conditions, positive-energy continuum states can be generated as easily as bound states.

In Section 2 the finite-difference approximation to the two-center Schrödinger equation is derived. A generalized Newton–Raphson iterative method for solving the system of finite-difference equations is presented in Section 3 and in Section 4 the results of two example calculations are presented, one of which is a continuum state.

2. Finite-Difference Approximation to Schrödinger's Equation

The two-center electronic wavefunction with nuclear charges Z_a and Z_b separated by a distance R can be rigorously factored into the form

$$\psi = L(\lambda)\, M(\mu)(e^{im\phi}/(2\pi)^{1/2}), \qquad m = 0, \pm 1, \ldots, \tag{1}$$

where λ, μ, and ϕ are the usual confocal elliptical coordinates

$$(\lambda = (r_a + r_b)/R, \qquad \mu = (r_a - r_b)/R).$$

The functions L and M are solutions of

$$\left[\frac{d}{d\lambda}(\lambda^2 - 1)\frac{d}{d\lambda} + A + \frac{ER^2\lambda^2}{2} + R(Z_a + Z_b)\,\lambda - \frac{m^2}{\lambda^2 - 1}\right] L(\lambda) = 0, \qquad 1 \leqslant \lambda \leqslant \infty, \tag{2}$$

and

$$\left[\frac{d}{d\mu}(1 - \mu^2)\frac{d}{d\mu} - A - \frac{ER^2\mu^2}{2} - R(Z_a - Z_b)\,\mu - \frac{m^2}{1 - \mu^2}\right] M(\mu) = 0, \qquad -1 \leqslant \mu \leqslant +1. \tag{3}$$

Equations (2) and (3) are to be solved subject to the following conditions.

(i) boundary conditions: $L(\infty) = 0$ and $L(1)$, $M(-1)$, and $M(+1)$ must be finite. (4)

(ii) normalization conditions:

$$\frac{R^3}{8} \int L^2 M^2 (\lambda^2 - \mu^2)\, d\lambda\, d\mu = 1, \tag{5}$$

$$\int M^2\, d\mu = 1. \tag{6}$$

The condition (6) is required in order to determine L and M uniquely, because (2) and (3) are homogeneous and (5) alone is satisfied by all functions $L' = \alpha L$, $M' = (1/\alpha) M$, where α is an arbitrary constant.

We proceed now to determine finite-difference equations which are approximations to the differential equations and normalization conditions, (2), (3), (5), and (6). The boundary conditions (4), however, are not in a form that can be treated easily, and it is useful first to make the following transformations, originally used by Jaffé [2]:

$$X \equiv (\lambda^2 - 1)\, L, \tag{7}$$

$$Y \equiv (1 - \mu^2)\, M, \tag{8}$$

$$\xi \equiv (\lambda - 1)/(\lambda + 1), \qquad 0 \leqslant \xi \leqslant 1. \tag{9}$$

In terms of the ξ and μ independent variables the differential equations (2) and (3) become

$$\left[\xi(1-\xi)^2 \frac{d^2}{d\xi^2} - (1 + 2\xi - 3\xi^2) \frac{d}{d\xi} + A + \frac{ER^2}{2}\left(\frac{1+\xi}{1-\xi}\right) + R(Z_a + Z_b)\left(\frac{1+\xi}{1-\xi}\right) - \frac{m^2(1-\xi)^2}{4\xi} + \frac{1+\xi^2}{\xi}\right] X(\xi) = 0, \tag{10}$$

$$\left[(1-\mu^2)\frac{d^2}{d\mu^2} + 2\mu \frac{d}{d\mu} - A - \frac{ER^2\mu^2}{2} - R(Z_a - Z_b)\,\mu - \frac{m^2}{1-\mu^2} + \frac{2(1+\mu^2)}{1-\mu^2}\right] Y(\mu) = 0, \tag{11}$$

while the normalization conditions (5) and (6) become

$$\frac{R^3}{64} \int \frac{[((1+\xi)/(1-\xi))^2 - \mu^2]\,(1-\xi)^2\, X(\xi)^2\, Y(\mu)^2\, d\xi\, d\mu}{\xi^2(1-\mu^2)^2} - 1 = 0, \tag{12}$$

and

$$\int \frac{Y(\mu)^2}{(1-\mu^2)^2}\, d\mu - 1 = 0. \tag{13}$$

The two-point boundary conditions on $X(\xi)$ and $Y(\mu)$ are now simply

$$X(0) = X(1) = 0, \tag{14}$$

$$Y(-1) = Y(1) = 0. \tag{15}$$

These transformations (7), (8) and (9) offer the following advantages. The range of the new variable ξ is finite (0–1) and can be spanned by a finite mesh of equally spaced points. Also, the new boundary conditions (14) and (15) are easily incorporated into a system of finite-difference equations. Furthermore, a constant density of mesh points in ξ corresponds to a greater density in λ in the important region close to the internuclear axis, as opposed to the less important region far out.

We now translate the new system of equations (10) through (15) into finite-difference form. The ξ axis between $\xi = 0$ and $\xi = 1$ is divided by a mesh of $N_1 - 1$ evenly spaced internal points, and the interval between points is $h_1 = 1/N_1$. Likewise the μ axis between $\mu = -1$ and $\mu = +1$ is divided by a mesh of $N_2 - 1$ evenly spaced internal points, giving an interval of $h_2 = 2/N_2$. The following notation will be used:

$$\begin{aligned} \xi_k &= kh_1, \qquad k = 0, 1, \ldots, N_1, \\ X_k &= X(\xi_k), \\ \mu_k &= -1 + kh_2, \qquad k = 0, 1, \ldots, N_2, \\ Y_k &= Y(\mu_k). \end{aligned} \tag{16}$$

A first-order approximation to the derivatives in (10) and (11) is used. Explicitly at mesh point k,

$$\begin{aligned} \left.\frac{dX}{d\xi}\right|_{\xi_k} &\approx \frac{1}{2h_1}(X_{k+1} - X_{k-1}), \\ \left.\frac{d^2X}{d\xi^2}\right|_{\xi_k} &\approx \frac{1}{h_1^2}(X_{k-1} - 2X_k + X_{k+1}), \end{aligned} \tag{17}$$

and the same approximations are used for derivatives of Y. The integrals (12) and (13) are approximated by trapezoidal rule which is entirely consistent with the first-order approximations of the derivatives.

Writing the finite-difference approximation to (10) and (11) at each internal mesh point we have the following set of equations:

$$\left[-\frac{2(1-kh_1)^2}{h_1}+A+\frac{ER^2}{2}\left(\frac{1+kh_1}{1-kh_1}\right)^2+R(Z_a+Z_b)\left(\frac{1+kh_1}{1-kh_1}\right)\right.$$
$$\left.-\frac{m^2(1-kh_1)^2}{4kh_1}+\frac{1+k^2h_1^2}{kh_1}\right]X_k+\frac{k(1-kh_1)^2}{h_1}(X_{k-1}-X_{k+1})$$
$$+\frac{(1-2kh_1+3k^2h_1^2)}{2h_1}(X_{k-1}-X_{k+1})=0, \qquad k=1,\ldots,N_1-1, \tag{18}$$

$$\left[-\frac{2k(2-kh_2)}{h_2}-A-\frac{ER^2}{2}(kh_2-1)^2-R(Z_a-Z_b)(kh_2-1)\right.$$
$$\left.-\frac{m^2}{kh_2(2-kh_2)}+\frac{2(2-2kh_2+k^2h_2^2)}{kh_2(2-kh_2)}\right]Y_k+\frac{k(2-kh_2)}{h_2}$$
$$\times(Y_{k-1}-Y_{k+1})-\frac{(kh_2-1)}{h_2}(Y_{k-1}-Y_{k+1})=0,$$
$$k=1,\ldots,N_2-1. \tag{19}$$

The normalization conditions (12) and (13) are approximated by

$$\frac{R^3}{64}\sum_{j=1}^{N_1-1}\sum_{k=1}^{N_2-1}\frac{[((1+jh_1)/(1-jh_1))^2-(kh_2-1)^2](1-jh_1)^2}{j^2h_1k^2h_2(2-kh_2)^2}X_j^2Y_k^2-1=0, \tag{20}$$

$$\sum_{k=1}^{N_2-1}\frac{Y_k^2}{k^2h_2(2-kh_2)^2}-1=0, \tag{21}$$

while the boundary conditions (14) and (15) translate into

$$X_0=X_{N_1}=0 \tag{22}$$

and

$$Y_0=Y_{N_2}=0. \tag{23}$$

These equations (18)–(23) are a set of nonlinear algebraic equations in the unknowns X_k ($k=0,\ldots,N_1$), Y_k ($k=0,\ldots,N_2$), the energy E, and the separation constant A. In the next section we give a practical method for solving this system.

3. Method of Solution

The finite-difference system comprises N_1+N_2+4 equations in as many unknowns. We can immediately substitute the boundary conditions (22) and (23) into equations (18) and (19) for $k=1$ and N_1-1 and $k=1$ and N_2-1

respectively. In so doing we have reduced the order of our system of equations (and unknowns) by 4, and the two-point boundary conditions (22) and (23) will be automatically satisfied.

Before introducing a Newton–Raphson algorithm for solving the system, it is most convenient to alter the notation slightly. It is desirable to think of all the unknowns, the X_k, Y_k, E and A, on equal footing. With this goal in mind we make the following definitions:

$$X_{k+N_1-1} \equiv Y_k, \qquad k = 1,..., N_2 - 1, \tag{24}$$

$$X_{N_1+N_2-1} \equiv A, \tag{25}$$

$$X_{N_1+N_2} \equiv E. \tag{26}$$

We note in passing that the definition (24) ($k = 1$) has nothing whatsoever to do with the boundary condition (22). X_{N_1} has been discarded from the list of unknowns, and we are merely reusing the symbol.

Now that we have all the unknowns notationally on the same footing, we simply number the equations 1 to $N_1 + N_2$, first taking (18) ($k = 1,..., N_1 - 1$), then (19) ($k = 1,..., N_2 - 1$), and finally (20) and (21). In the revised notation this system can be represented formally as

$$f_k(X_1 X_2 \cdots X_{N_1+N_2}) = 0, \qquad k = 1,..., N_1 + N_2, \tag{27}$$

where the equations for $k \leqslant N_1 - 1$ represent (18), those for $N_1 \leqslant k \leqslant N_1 + N_2 - 2$ represent (19), and $k = N_1 + N_2 - 1$ corresponds to (21) and $k = N_1 + N_2$ to (20).

The equations (27) are a set of nonlinear algebraic equations, and, starting with an initial approximation, can be solved by means of a generalized Newton–Raphson iterative method [8]. Let $\mathbf{X}^{(n)} \equiv (X_1^{(n)} \cdots X_{N_1+N_2}^{(n)})$ be a vector whose components are the values of the unknowns in (27) at the nth iteration, and also define $\mathbf{F}^{(n)} \equiv (f_1(\mathbf{X}^{(n)}),..., f_{N_1+N_2}(\mathbf{X}^{(n)}))$. Then at the $(n + 1)$th iteration the solution vector is given in terms of values at the nth iteration by

$$\mathbf{X}^{(n+1)} = \mathbf{X}^{(n)} - (J^{(n)})^{-1} \mathbf{F}^{(n)}, \tag{28}$$

where J is a Jacobian matrix, the elements of which are

$$J_{lm}^{(n)} \equiv \left(\frac{\partial f_l}{\partial X_m}\right)^{(n)}. \tag{29}$$

The iteration (28) is repeated until

$$\max(|f_1(\mathbf{X}^{(n)})|,..., |f_{N_1+N_2}(\mathbf{X}^{(n)})|) \leqslant \text{tolerance}, \tag{30}$$

since when $\mathbf{F}^{(n)} = 0$ the system of finite-difference equations is solved exactly.

A very efficient algorithm for the rapid solution of (28) has been described in a previous paper [8]. It is based upon the special form of the Jacobian matrix. Because the equations (27) only involve the X's at neighbouring mesh points (X_{k-1}, X_k, and X_{k+1}), the matrix is sparse and in almost tridiagonal form.

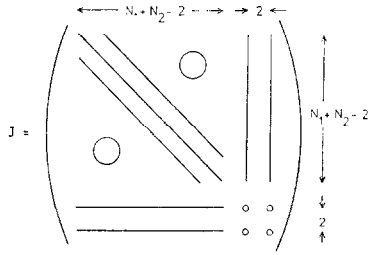

(31)

The two nonzero rows and columns in J are due respectively to the presence of all the X's except $X_{N_1+N_2-1}$ and $X_{N_1+N_2}$ in the last two equations of (27) and the presence of $X_{N_1+N_2-1}$ and $X_{N_1+N_2}$ in the rest of equations (27). With the J matrix of this form (28) can be rapidly solved by means of a partitioning [8].

It remains to determine a starting vector $\mathbf{X}^{(0)}$ for the algorithm. In the united-atom limit ($R = 0$) the hydrogenic functions ($Z = Z_a + Z_b$) solve the problem. One starts the molecular calculation, therefore, at small R (but not zero) using a hydrogenic wavefunction in finite difference form (in terms of ξ and μ) as the starting vector $\mathbf{X}^{(0)}$. Which one of the molecular eigenstates is converged upon depends upon which hydrogenic wavefunction is used (and also the value of m in (18) and (19)). To obtain the solution for all values of R a tracking procedure is employed where the converged solution for one value of R is used as a starting vector for a larger value of R. Since in general one is interested in the electronic energy as a function of R the whole tracking procedure provides useful information.

4. Results of Calculations

To illustrate the accuracy and practicality of the algorithm just described we present the results of two example calculations. The first is the $2s\sigma_g$ state of H_2^+ ($Z_a = Z_b = 1$) and the second is a σ_g continuum state of H_2^+.

Of course for any finite values of h_1 and h_2 we have only an approximate solution of Schrödinger's equation. One can improve the accuracy by taking more mesh points, but roundoff error increases with the number of mesh points. Instead we make an extrapolation to the $h_1 = h_2 = 0$ limit based on a number of calculations at different finite values of h_1 and h_2. The result is a two-dimensional generalization of Richardson h^2 extrapolation [9].

Let Φ denote any scalar quantity (or more generally an element of a tensor) which depends upon one or more of the finite difference solutions of Schrödinger's equation. For example Φ could be the electronic energy, the separation constant, or a matrix element of any tensor operator. Considering Φ to be a continuous function of the mesh spacings h_1 and h_2, we expand it in Taylor series about the point $h_1 = h_2 = 0$. However, since inverting the coordinate system, corresponding to $h_1 \to -h_1$ and $h_2 \to -h_2$, cannot change the resulting value of Φ, we can omit all terms in the expansion containing odd powers of h_1 and/or h_2. To sixth order, therefore, we have

$$\Phi(h_1 h_2) = a_1 + a_2 h_1^2 + a_3 h_2^2 + a_4 h_1^4 + a_5 h_2^4 + a_6 h_1^2 h_2^2 + a_7 h_1^6 + a_8 h_2^6 + a_9 h_1^2 h_2^4 + a_{10} h_1^4 h_2^2 + \cdots, \tag{32}$$

where $a_1 \equiv \Phi(0, 0)$, $a_2 \equiv \partial^2\Phi/\partial h_1^2 \,|_0$, etc. For an order h^2 extrapolation we need three points, for h^4 six, for h^6 ten, etc.

Define the vectors $\mathbf{\Phi} \equiv (\Phi(h_1^{(1)} h_2^{(1)}), \Phi(h_1^{(2)} h_2^{(2)}), \ldots)$, where $(h_1^{(i)}, h_2^{(i)})$ are different sets of values of h_1 and h_2, and $\mathbf{A} \equiv (a_1, a_2, \ldots)$, the dimension of the vectors depending upon the order of the extrapolation. Then

$$\mathbf{A} = H^{-1}\mathbf{\Phi}, \tag{33}$$

where the ith row of the H matrix is $(1, h_1^{(i)^2}, h_2^{(i)^2}, \ldots)$. The first element of the **A** vector is the extrapolated value of Φ. The remaining elements of A are useful in ascertaining the reliability of the extrapolation.

We have carried out a series of h^2, h^4, and h^6 extrapolations on the energy of the $2s\sigma_g$ state of H_2^+ at $R = 5.0$ AU, and the results are presented in Table I in the form of a generalized Neville table [10]. In the table the first two columns give the values of h_1 and h_2, respectively, while the third column gives the corresponding value of the energy. The fourth column gives the first-order extrapolants, each based upon three points, including the one opposite the entry in column 3 and one on either side. The fifth column gives the second-order extrapolants, each based upon six points, including the three on either side of the position opposite the entry in column 5. Finally the sixth column gives the third-order extrapolants, each based upon ten points in the same manner. The internal agreement of the various extrapolants gives an indication of the accuracy. Thus while the raw data is only accurate to three significant figures the third-order extrapolants are accurate to eight.

We have also performed these same extrapolations on the energy of a σ_g continuum state of H_2^+ at $R = 5.0$ AU. But before we present these results we should explain how these states are obtained, how they can be classified, and how they can be used. First, since the continuum states have no exponential

TABLE I

Generalized Neville Table for the Energy of the $2s\sigma_g$ state of H_2^+ at $R = 5.0$ AU[a]

h_1	h_2	Zeroth order extrapolant	First order extrapolant	Second order extrapolant	Third order extrapolant
0.01234568	0.02469136	−1.1026582			
0.01234568	0.01652893	−1.1034901	−1.1025967		
0.00826446	0.02469136	−1.1017924	−1.1028660		
				−1.1026218	
0.01234568	0.01242236	−1.1038203	−1.1024840		
				−1.1026213	
0.00621118	0.02469136	−1.1014599	−1.1025791		
				−1.1026213	−1.1026276
0.00826446	0.01652893	−1.1026227	−1.1025312		
				−1.1026214	−1.1026276
0.00621118	0.01652893	−1.1022897	−1.1026149		
				−1.1026287	
0.00826446	0.01242236	−1.1029524	−1.1026146		
				−1.1026264	
0.00684932	0.01315789	−1.1026534	−1.1026212		
0.00662252	0.01282051	−1.1026509	−1.1026217		
0.00621118	0.01242236	−1.1026191			

[a] Energies are in atomic units (AU).

tail but oscillate to infinity, it is clear that one cannot hope to represent these functions by a finite number of mesh points in the ξ space as defined by (9). However, if we truncate our ξ space such that $0 < \xi < b$ where $b < 1$, then over this range of ξ a continuum state will have a finite number of oscillations. Furthermore, if we change the boundary condition (14) to read

$$X(0) = X(b) = 0, \qquad b < 1, \tag{34}$$

then we can obtain that particular continuum state with a node at $\xi = b$.

One might raise the objection that this is not a continuum state but in fact a bound state confined to a finite ellipsoidal box. Actually for all positive values of energy, there is absolutely no difference between the two wavefunctions. They are merely two different ways of looking at the same thing. Over the range $0 < \xi < b$ the wavefunction satisfies Schrödinger's equation with positive energy

and a node occurs at the boundary. In fact the parts of the wavefunction of a given continuum state in the range from $\xi = 0$ out to each successive node at $\xi = b_n$ $(n = 1, 2, \ldots, \infty)$ are equivalent respectively, within a normalization factor, to a sequence of bound states, each successive member of which has been compressed to the range $0 < \xi < b_n$ $(n = 1, 2, \ldots, \infty)$, where b_n approaches 1 as $n \to \infty$.

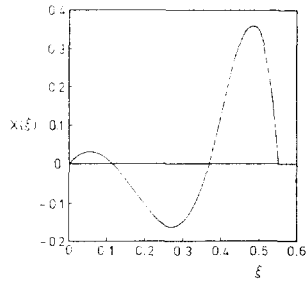

FIG. 1. Wavefunction of the $3s\sigma_g(0.55)$ continuum state of H_2^+ at $R = 5.0$ AU.

For example, in Fig. 1 we show a plot of $X(\xi)$ against ξ $(0 < \xi < 0.55)$ for a continuum state of positive energy (≈ 0.133 AU) which has a node at $\xi = 0.55$. This state was obtained by compressing the $3s\sigma_g$ bound state into the region $0 < \xi < 0.55$ by means of a tracking procedure. As the state is compressed the energy increases from -0.142 AU for $b = 1$ to $+0.133$ AU when $b = 0.55$. It is interesting to note that in the tracking when the energy is negative $X(\xi)$ has positive curvature near $\xi = b$ which is characteristic of the exponential tail of a bound state, but as soon as the energy goes positive the curvature goes to zero at $\xi = b$, and this corresponds to the node of a continuum state. In the figure the part of the wavefunction out to the second node at $\xi = 0.368$ corresponds to the $2s\sigma_g$ state compressed to this region, while the part out to the first node corresponds to the compressed $1s\sigma_g$ state. In general the compressed $ns\sigma_g$ state corresponds to n oscillations of the continuum state out to $\xi = b_n$.

Since the continuum is known to make a significant contribution in many problems, one would like to employ these continuum states as elements of basis sets containing mostly bound states. This can be accomplished with a small and controllable error introduced, if b is chosen large enough such that the overlap of the continuum states with bound states and with each other in the region $b < \xi < 1$ is small because of the exponential tail of the bound states and the rapid oscillations of the continuum states in this region.

One can classify a continuum state by energy and angular momentum, but in view of the application just suggested it might be more useful to associate a continuum state with a compressed bound state of equivalent energy while stating

TABLE II

Generalized Neville Table for the Energy of the $3s\sigma_{gc}(0.55)$ Continuum State of H_2^+ at $R = 5.0$ AU[a]

h_1	h_2	Zeroth order extrapolant	First order extrapolant	Second order extrapolant	Third order extrapolant
0.00539216	0.01980198	0.13254956			
0.00450820	0.01652893	0.13266980	0.13295300		
0.00433071	0.01587302	0.13269144	0.13295326		
				0.13295446	
0.00416667	0.01526718	0.13271070	0.13295341		
				0.13295449	
0.00387323	0.01418440	0.13274334	0.13295353		
				0.13295451	0.13295467
0.00374150	0.01369863	0.13275725	0.13295364		
				0.13295453	0.13295467
0.00361842	0.01324503	0.13276983	0.13295371		
				0.13295455	
0.00350318	0.01282051	0.13278123	0.13295377		
				0.13295456	
0.00339506	0.01242236	0.13279161	0.13295383		
0.00329341	0.01204819	0.13280107	0.13295389		
0.00319767	0.01169591	0.13280974			

[a] Energies are in atomic units (AU).

the region of ξ that is being included. In this way the state plotted in Fig. 1 could be labelled $3s\sigma_{gc}(0.55)$ where the c stands for compressed.

Finally in Table II we present the extrapolated energy for the $3s\sigma_{gc}(0.55)$ state in the same form as Table I. The accuracy in this case is similar.

5. Conclusions

A relatively simple and efficient finite-difference algorithm for solving the two-center Schrödinger equation has been presented. The resulting energies and wavefunctions for H_2^+ certainly do not compete with the series method in terms of accuracy. (Peek [6] has obtained an accuracy of $1 : 10^{17}$ with 20 terms in μ and 16 terms in λ). Although greater accuracy could be obtained by going to a

higher-order difference formula, nevertheless the eight significant figure accuracy achieved with the present first-order approximation is sufficient for most purposes.

The present algorithm has been used to generate H_2^+ wavefunctions over a range of nuclear separations from near zero out to 50 AU, a solution at one separation being rapidly tracked into another. For an optimum distribution of mesh points at large separations one can employ a transformation

$$\xi = \frac{\lambda - 1}{c\lambda + 1}, \tag{35}$$

with $c \gg 1$ instead of (9). Also single-electron diatomic orbitals have been generated for LiH^{3+} and Li_2^{5+} with no deterioration in the convergence properties of the algorithm.

Because of the flexibility and versatility of the algorithm the resulting numerical diatomic orbitals should prove to be useful as basis functions in calculations of stationary molecular electronic states as well as separation-dependent basis functions for atom–atom collisions.

Note added in proof. The normalization conditions in trapezoidal rule (20) and (21) need endpoint corrections to be entirely correct, and these cannot be expressed in a very concise manner. For example, the trapezoidal rule approximation (21) would be correct if the integrand of (13) went to zero at the endpoints $\mu = \pm 1$. Although $Y(-1) = Y(1) = 0$, the indeterminate form $Y(\mu)/(1 - \mu^2) = M(\mu)$ goes to a finite value at the endpoints. Therefore (21) needs an additional term $h_2(M_0^2 + M_{N_2}^2)/2$, but since M_0 and M_{N_2} are not in the set of finite-difference variables this term poses a problem. One solution is to express M_0 and M_{N_2} in terms of second-order Taylor expansions about the first and $N_2 - 1$ mesh points, respectively, using (8) to express M and its derivatives in terms of Y and its derivatives, and using (17) to approximate the derivatives of Y at the first and $N_2 - 1$ mesh points. Similar considerations must be brought to bear on (20). In particular note that $L(\lambda = 1)$ is not necessarily zero.

REFERENCES

1. Ø. BURRAU, *Kungl. Danske Videnskab Mat.-Fys. Medd.* **7** (1927), 1.
2. G. JAFFÉ, *Z. Physik* **87** (1934), 535.
3. D. R. BATES, K. LEDSHAM, AND G. L. STEWART, *Phil. Trans. Roy. Soc. London Ser. A* **246** (1953), 215.
4. R. F. WALLIS AND H. M. HULBURT, *J. Chem. Phys.* **22** (1954), 774.
5. H. WIND, *J. Chem. Phys.* **42** (1965), 2371.
6. J. M. PEEK, *J. Chem. Phys.* **43** (1965), 3004.
7. C. T. LLAGUNO, S. K. GUPTA, AND S. M. ROTHSTEIN, *Int. J. Quant. Chem.* 7 (1973), 819.
8. J. K. CAYFORD, W. R. FIMPLE, AND D. G. UNGER, *J. Comp. Phys.* **15** (1974), 81.
9. L. F. RICHARDSON, *Phil. Trans. Roy. Soc. London Ser. A* **226** (1927), 299; Z. KOPAL, "Numerical Analysis," Section V-C, Wiley, New York, 1961.
10. E. H. NEVILLE, *J. Indian Math. Soc.* **20** (1934), 87.